Translational dynamics of a particle with anchored chains in entangled polymers

W. Sung and Min Gyu Lee
Department of Physics, Pohang University of Science and Technology, Pohang, 790-600, Korea
(Received 13 May 1994)

We investigate the dynamics of a spherical particle of an arbitrary size immersed in entangled linear polymers. In particular, we calculate analytically and numerically the velocity autocorrelation function (VAF) of the particle, using the microscopic boundary layer model developed by Sung [*Physics of Complex Fluids and Biological Systems,* edited by W. Sung *et al.* (Min Eum Sa Co, Seoul, 1993)]. The model incorporates the short-range dynamical effect of the interface chains attached to the particle and simultaneously entangled with background chains, as well as the longer-range viscoelastic response from the background, treated as a continuum. The VAF calculated therefrom manifests the interplay of elastic response at short times and viscous relaxation via chain reptation at long times. The VAF at long times decays very slowly with the long-time tails suppressed due to the entanglement constraint. On the other hand, the constraint gives rise to an elastic response at short times, leading to enhanced caging of the particle. We discuss the various modes of the particle dynamics that emerge as the particle size varies.

PACS number(s): 61.41.+e, 66.10.−x, 83.10.Nn, 83.20.Lr

I. INTRODUCTION

The entangled linear polymers either in melt or solution are characterized by an enormously slow relaxation. This mode of slow dynamics is *reptation,* a large-scale diffusion of the polymers in snakelike fashion along their contours, by which the chains can be disengaged from the entanglements [1,2]. The relaxation time τ_D, also called the reptation time, goes like $\tau_D \propto N^{\delta}$ ($\delta=3$, theory; $\delta=3.4$, experiment), where N is the number of Kuhn segments each of length b in a chain. For times much longer than τ_D, the polymers flow as a liquid, while for times much shorter than τ_D, they respond as an elastic solid since each polymer remains caged to the neighboring chains due to the entanglements. Depending upon the chain length, the fascinating manifestation of this molecular viscoelasticity can be observed on a macroscopic time scale.

Now suppose that a particle is introduced into the long entangled polymers with some chains anchored on its surface. Then the particle motion is influenced by its neighboring chains instantly and also by the viscoelastic response of the more distant background polymers subsequently. We pose these questions: How is the translational motion of the particle described on various time scales? How does the motion depend upon particle size, polymer molecular weight, and degree of chain anchorage on the particle surface? These questions, let alone their scientific significance, are relevant to many practical situations including the industrial processing of particle-polymer compounds.

We endeavor, in this paper, to answer the questions posed above in an analytic manner by calculating the velocity autocorrelation function (VAF) of the particle. To this end, we employ a *microscopic boundary layer* (MBL) *model* [3] recently developed by us to investigate steady-state particle diffusion in polymer liquids. The model, a polymer-particle analogue of the Bethe-Peierls model [4], describes the short-range interaction between particle and the chains in its immediate neighborhood microscopically using chain statistical dynamics, while it treats all the distant chains as a continuum responding to the particle motion hydrodynamically. The hydrodynamic response is then calculated in a way consistent with the generalized boundary condition it must meet on the outer surface of the boundary layer. We found that in an earlier work the model reasonably yields the steady-state particle diffusivity to be given as a sum of two contributions, one from disengagement of the anchored chains and the other from hydrodynamic feedback of the distant chains [5]. In order to study the underlying dynamics, we will focus upon the velocity autocorrelation function of the particle for times ranging from a short time τ_e denoting the onset of the entanglement constraints [2] to long times larger than τ_D. We will consider a spherical particle of an arbitrary radius R and entangled polymers of monodisperse chain length, which is also arbitrary. We will confine ourselves here to the polymers in melt, nevertheless, adaptation of the theory to solutions is possible to the limited cases in which solvent effect is negligible or easy to incorporate.

Our presentation of the paper is as follows: In Sec. II, we recapitulate the basic elements of the microscopic boundary layer model developed earlier and generalize the model to accommodate the dynamic (nonsteady) situations we consider here. In Sec. III, we present the time-dependent generalized hydrodynamics of the polymer liquid treated as a viscoelastic continuum. We then solve the coupled hydrodynamic equations that satisfy the generalized boundary condition and obtain the VAF, which will be discussed in depth in Sec. IV. The results are summarized in Sec. V.

II. MICROSCOPIC BOUNDARY LAYER AND GENERALIZED BOUNDARY CONDITION

Here we summarize briefly the essential ingredients of the microscopic boundary layer (MBL) model developed earlier by us [3,5] and introduce the basic parameters for use in subsequent theoretical development. Also, we incorporate anew the effect of the chain disengagement into the generalized boundary condition, which is our main machinery for implementing viscoelastic response of polymers.

In the MBL model, the dynamic effect of chains on the particle is predominantly due to the *elastically effective surface chains* (ESCs) which are defined as those anchored on the particle at one end, and entangled, for the first time, with the background chains at the other (Fig. 1). Since the ESCs exclude other types of chains, we model an ESC as a random walk that starts at a point $\mathbf{r}_0 = R\hat{\mathbf{n}}_0$ on the particle surface (R is the particle radius) and terminates at the first entanglement without crossing the surface on the way. The statistics of this particle-avoiding walk was calculated assuming the ideality of the chain and using the image method [3]. The end-to-end distance probability density of the ESC with N_S segment each with length b is given by

$$P_{N_s} \propto (r^2 - R^2)\exp[-R_s^{-2}(\mathbf{r}-\mathbf{r}_0)^2] , \tag{1}$$

where $R_s \equiv \sqrt{(2N_s b^2)/3}$ is a length characteristic of the ESC, and $\mathbf{r}$ is the position of the entanglement from the center of the particle.

We define the width a of the boundary layer to be the most probable distance between the two ends of an ESC (Fig. 1), i.e., $a = |\mathbf{r}^*| - R$, where $\mathbf{r}^*$ is the $\mathbf{r}$ at which the probability is at maximum. It is given by

$$\left[\frac{a}{R_s}\right]^2 (a+2R) - (a+R) = 0 . \tag{2}$$

The a does not vary appreciably with R when $R > 10R_s$ and approaches to the asymptotic value $a \to (1/\sqrt{2})R_s$ as $R \to \infty$. Also, we obtain from the probability of an ESC the entropic chain force $\mathbf{f}_S$ necessary to extend its end by an increment $\delta\mathbf{x}$ away from the average separation

$$\begin{aligned} \mathbf{f}_S &= -k_B T \nabla \ln P_{N_S}(\mathbf{r}) \\ &= -\overleftrightarrow{\mathbf{K}} \cdot \delta\mathbf{x} . \end{aligned} \tag{3}$$

Here $\overleftrightarrow{\mathbf{K}}$ is the anisotropic spring constant tensor given by [5]

$$\begin{aligned} \overleftrightarrow{\mathbf{K}} &= k_B T [\nabla\nabla \ln P_{N_s}(\mathbf{r})]_{\mathbf{r}=\mathbf{r}^*=(R+a)\hat{\mathbf{n}}_0} \\ &= K_0 \overleftrightarrow{\mathbf{1}} + K_1 \hat{\mathbf{n}}_0 \hat{\mathbf{n}}_0 , \end{aligned}$$

with

$$K_0 = \frac{2k_B T}{R_s^2}\frac{R}{R+a} , \tag{4a}$$

$$K_1 = \frac{4k_B T}{R_s^2}\left[\frac{a}{R_s}\right]^2 . \tag{4b}$$

In the case of a large particle in which $R \gg R_s$, or $R \gg a$,

$$K_0 \simeq K_1 = \frac{2k_B T}{R_s^2} \equiv K . \tag{5}$$

Another important parameter in the model is the α, the number of ESCs per unit area of the outer boundary surface S_0, given by $r = R + a$. The α, presumed to be an independent variable, is fixed as a constant for simplicity in our problem here.

In terms of these parameters, the force per unit area on the particle by the ESCs drawn by $\delta\mathbf{x}$ is given by

$$\mathcal{F} = \alpha \overleftrightarrow{\mathbf{K}} \cdot \delta\mathbf{x} . \tag{6}$$

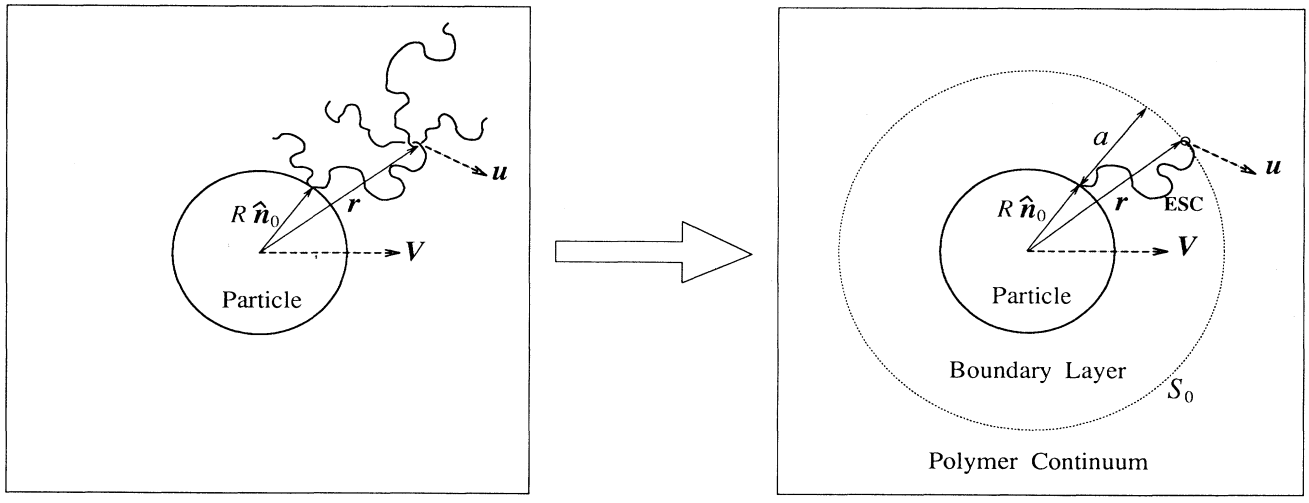

FIG. 1. A schematic picture of the boundary layer model and an effective surface chain (ESC) which is attached on the surface and entangled with a background chain during the reptation time. The a is the boundary layer size and S_0 is the outer boundary.

This is the case with the static situation wherein the particle is stationary with the chain anchored and entangled permanently. But with the particle set into motion with an average velocity $\bar{\mathbf{V}}(t)$ and the entanglement (link) with the background chains at $r=R+a$ released while moving with an average velocity $\mathbf{u}(t)$ (Fig. 1), Eq. (6) is modified to

$$\mathcal{F}(t)=\alpha\vec{\vec{\mathbf{K}}}\cdot\int_0^t dt'\psi(t-t')[\mathbf{u}((R+a)\hat{\mathbf{n}},t')-\bar{\mathbf{V}}(t')] . \quad (7)$$

Here $\psi(t)$ is the memory function descriptive of disengagement of the background chains. We assume in consistency with our boundary model elaborated below that the $\psi(t)$ is the average portion of a chain in bulk that remains at the time t in its initial entanglement constraints, as is given by the theory of Doi and Edwards [2]:

$$\psi(t)=\sum_{p=1}^{\infty}\frac{8}{p^2\pi}\exp\left[-\frac{p^2t}{\tau_d}\right] . \quad (8)$$

Here the p runs over odd integers, and

$$\tau_d=\frac{\zeta_1 N^3 b^4}{\pi^2 k_B T R_e^2} \quad (9)$$

is the largest reptational relaxation time, ζ_1 is the Rouse friction coefficient on a segment, N is the number of segments per polymer, and R_e is the (primitive) chain length between adjacent entanglements. All the parameters involved in Eq. (9) pertain to chains in the bulk.

To further clarify the meaning of Eq. (7), consider the short time ($t\ll\tau_d$) at which the ESC remains engaged with a background chain. At this short time, $\psi(t)\simeq 1$ and Eq. (7) can be read as the elastic force

$$\mathcal{F}\simeq\alpha\vec{\vec{\mathbf{K}}}\cdot\delta\mathbf{x}(t) , \quad (10)$$

with $\delta\mathbf{x}(t)=\int_0^t\mathbf{u}(t')dt'$ denoting the displacement by which the ESC is drawn. On the other hand, for long time, steady state, Eq. (7) is reduced to a frictional force

$$\mathcal{F}=\alpha\vec{\vec{\mathbf{K}}}\cdot\tau_D(\mathbf{u}-\bar{\mathbf{V}}) , \quad (11)$$

where τ_D is the relaxation time given by

$$\tau_D=\int_0^{\infty}\psi(t)dt=\frac{\pi^2}{12}\tau_d . \quad (12)$$

Equation (11) is the basic equation we used for calculating steady-state diffusion constant [3]. Since τ_D depends strongly upon N, namely, $\tau_D\sim N^3$ according to the theories of de Gennes [1] and Doi and Edwards [2] the frictional force on the particle is indeed dominated by ESCs (i.e., by entanglements) for long chains and is given by Eq. (11). Evidently, Eq. (7) interpolates the extremes of elastic and viscous forces and, of course, display the intermediate viscoelastic behavior that depends upon the time scale of the particle motion.

The validity of the force, Eq. (7), is restricted to $t>\tau_e$, with τ_e denoting the time for onset of entanglement constraints. On the other hand, for times $t\lesssim\tau_e$, Rouse segmental friction on the particle together with other possible small molecular relaxation mechanisms should be included for the total friction on the particle. In development of our theory we confine ourselves to the case $t>\tau_e$ to assure that the ESCs play a dominant role in affecting dynamics of the particle.

In our MBL model, we treat the distant polymers beyond the boundary layer ($r>R+a$) as a viscoelastic continuum. With the continuum description extrapolated to the outer boundary S_0 (Fig. 1), the force per unit area on S_0 over the particle, then, is to be given by the hydrodynamic stress $-\vec{\vec{\sigma}}\cdot\hat{\mathbf{n}}$. In our model, this is equated to the chain dynamical force per unit area of S_0, Eq. (7)

$$\alpha\vec{\vec{\mathbf{K}}}\cdot\int_0^t dt'\psi(t-t')[\mathbf{u}((R+a)\hat{\mathbf{n}},t')-\bar{\mathbf{V}}(t')] = -\vec{\vec{\sigma}}((R+a)\hat{\mathbf{n}},t)\cdot\hat{\mathbf{n}} . \quad (13)$$

With the average velocity of entanglement (link) $\mathbf{u}$ at $\mathbf{r}=(R+a)\hat{\mathbf{n}}$ identified as the velocity $\mathbf{u}$ of the polymer continuum (at the same point) that appears in the stress tensor $\vec{\vec{\sigma}}((R+a)\hat{\mathbf{n}},t)$ [see Eq. (20)], Eq. (13) is regarded as the generalized boundary condition to be met by $\mathbf{u}$ on the outer boundary S_0. This equation provides a machinery to calculate the viscoelastic response of the background polymers to the particle motion, especially the velocity field $\mathbf{u}(\mathbf{r},t)$ in terms of the average particle velocity $\bar{\mathbf{V}}(t)$, incorporating the interface chain effect in a self-consistent way, as shown next.

III. VISCOELASTIC RESPONSE OF AN ENTANGLED POLYMER CONTINUUM TO THE PARTICLE MOTION

In this section, we present a set of coupled hydrodynamic equations for the viscoelastic polymer media in the linearized forms. And then we solve them using the generalized boundary condition, Eq. (13), for the frequency-dependent friction coefficient $\zeta(\omega)$ and finally the velocity autocorrelation function (VAF) $C(t)$ defined by Eq. (45).

In a low-wave number (hydrodynamic) description, the state of a fluid is completely specified by the hydrodynamic fields. With the fluctuation of temperature neglected, the fields are the mass density $\rho(\mathbf{r},t)$ and the fluid velocity $\mathbf{u}(\mathbf{r},t)$ which are coupled to one another by continuity equations

$$\frac{\partial}{\partial t}\rho(\mathbf{r},t)+\nabla\cdot\{\rho(\mathbf{r},t)\mathbf{u}(\mathbf{r},t)\}=0 , \quad (14)$$

$$\frac{\partial}{\partial t}\{\rho(\mathbf{r},t)\mathbf{u}(\mathbf{r},t)\}+\nabla\cdot\{\rho(\mathbf{r},t)\mathbf{u}(\mathbf{r},t)\mathbf{u}(\mathbf{r},t) +\vec{\vec{\sigma}}(\mathbf{r},t)\}=0 . \quad (15)$$

Since the linear transport—translational diffusivity in this case—is investigated, it suffices to consider the linearized version of the coupled equations for deviations from equilibrium

$$\delta\rho(\mathbf{r},t)=\rho(\mathbf{r},t)-\rho_{\text{eq}} , \quad (16)$$

$$\delta\mathbf{u}(\mathbf{r},t)=\mathbf{u}(\mathbf{r},t) , \quad (17)$$

which are

$$\frac{\partial}{\partial t}\delta\rho(\mathbf{r},t)+\rho_{\text{eq}}\nabla\cdot\mathbf{u}(\mathbf{r},t)=0 , \tag{18}$$

$$\rho_{\text{eq}}\frac{\partial}{\partial t}\mathbf{u}(\mathbf{r},t)+\nabla\cdot\vec{\sigma}(\mathbf{r},t)=0 . \tag{19}$$

Here ρ_{eq} is the equilibrium mass density of the fluid which will be denoted by ρ hereafter.

For Newtonian fluids, the stress tensor $\vec{\sigma}$ is given by the following constitutive equation:

$$\begin{aligned}\sigma_{ij}(\mathbf{r},t)=&\delta p(\mathbf{r},t)\delta_{ij}-\eta^B\nabla\cdot\mathbf{u}(\mathbf{r},t)\delta_{ij}\\&-\eta\{\nabla_i u_j(\mathbf{r},t)+\nabla_j u_i(\mathbf{r},t)\\&-\tfrac{2}{3}\nabla\cdot\mathbf{u}(\mathbf{r},t)\delta_{ij}\} ,\end{aligned} \tag{20}$$

where $\delta p(\mathbf{r},t)$ is the linear deviation of pressure and η and η^B are the constant shear and bulk viscosities. The fluid described on molecular relaxation times shows the viscoelastic behavior and then the stress in Eq. (20) is replaced by

$$\begin{aligned}\sigma_{ij}(\mathbf{r},t)=&\delta p(\mathbf{r},t)\delta_{ij}-\int_0^t dt'[\eta^B(t-t')\nabla\cdot\mathbf{u}(\mathbf{r},t')\delta_{ij}]\\&-\int_0^t dt'[\eta(t-t')\{\nabla_i u_j(\mathbf{r},t')+\nabla_j u_i(\mathbf{r},t')\\&-\tfrac{2}{3}\nabla\cdot\mathbf{u}(\mathbf{r},t')\delta_{ij}\}] ,\end{aligned} \tag{21}$$

where the shear- and bulk-relaxation modulus $\eta(t)$ and $\eta^B(t)$ can be given from molecular theories. For a liquid of entangled polymers, we employ the Doi-Edwards theory [2], according to which the shear-relaxation modulus is given by

$$\eta(t)=G\psi(t) , \tag{22}$$

where G is the plateau modulus and $\psi(t)$ is the reptational-relaxation function given earlier by Eq. (8). There seems to be no theory available, however, for the bulk-relaxation modulus, which has not been incorporated in most of the hydrodynamic calculations using the condition of incompressibility, $\nabla\cdot\mathbf{u}=0$. We need in our viscoelastic study of polymeric liquid to incorporate compressibility, which gives rise to a longitudinal sound mode. As discussed in the similar study by Zwanzig and Bixon [6] of the atomic VAF in simple fluids and as will be shown in this paper, this effect appears to be non-negligible. We assume that this relaxation occurs on a similar molecular mechanism, namely, reptation

$$\eta^B(t)=G^B\psi(t) . \tag{23}$$

Here G^B is the bulk modulus the system were to have if all the entanglements are replaced by permanent crosslinks.

At times much shorter than τ_D, the relaxation time of $\psi(t)$, Eq. (21) is replaced by

$$\begin{aligned}\sigma_{ij}(\mathbf{r},t)=&\delta p(\mathbf{r},t)\delta_{ij}-G^B\nabla\cdot\delta\mathbf{x}(\mathbf{r},t)\delta_{ij}\\&-G\{\nabla_i\delta x_j(\mathbf{r},t)+\nabla_j\delta x_i(\mathbf{r},t)\\&-\tfrac{2}{3}\nabla\cdot\delta\mathbf{x}(\mathbf{r},t)\delta_{ij}\} ,\end{aligned} \tag{24}$$

which is the relation between the stress and strain $\nabla\delta\mathbf{x}(\mathbf{r},t)$ ($\delta\mathbf{x}$ is the displacement) for an element in an elastic solid continuum. It is clear that, at such short times, the entanglements are not released but act as crosslinks, yielding the moduli G and G^B. Then, the coupled hydrodynamic equations become the wave equations for longitudinal and transverse sounds in the elastic solid.

In solving the viscoelastic hydrodynamic equations, it is convenient to use the Laplace transform

$$\mathbf{u}(\mathbf{r},\epsilon)=\int_0^\infty \mathbf{u}(\mathbf{r},t)e^{-\epsilon t}dt , \tag{25}$$

where $\epsilon\simeq -i\omega$ (apart from a small positive real part) in the language of the Fourier transformation

$$\mathbf{u}(\mathbf{r},\omega)=\int_{-\infty}^\infty \mathbf{u}(\mathbf{r},t)e^{i\omega t}dt . \tag{26}$$

The Laplace transforms of Eqs. (18) and (19) are

$$-\epsilon\delta\rho(\epsilon)=\rho\nabla\cdot\mathbf{u}(\mathbf{r},\epsilon) \tag{27}$$

$$\begin{aligned}\rho\epsilon\mathbf{u}(\mathbf{r},\epsilon)=&\left\{\frac{\rho c^2}{\epsilon}+\frac{4}{3}\eta(\epsilon)+\eta^B(\epsilon)\right\}\nabla\nabla\cdot\mathbf{u}(\mathbf{r},\epsilon)\\&-\eta(\epsilon)\nabla\times\nabla\times\mathbf{u}(\mathbf{r},\epsilon) ,\end{aligned} \tag{28}$$

where we assumed that the fields (deviations) are zero at $t=0$, i.e., that the fluid is at equilibrium initially and used the relation

$$\nabla\delta p(\mathbf{r},t)=\left[\frac{\partial p}{\partial\rho}\right]_T\nabla\delta\rho(\mathbf{r},t)=c^2\nabla\delta\rho(\mathbf{r},t) , \tag{29}$$

with $c=\sqrt{(\partial p/\partial\rho)_T}$ denoting isothermal sound velocity.

Taking a divergence, and then a curl on Eq. (28), we can decouple the longitudinal velocity field $g_l\equiv\nabla\cdot\mathbf{u}$ from the transverse field $\mathbf{g}_t\equiv\nabla\times\mathbf{u}$ to have

$$\nabla^2 g_l(\mathbf{r},\epsilon)=k_l^2 g_l(\mathbf{r},\epsilon) , \tag{30}$$

$$\nabla^2\mathbf{g}_t(\mathbf{r},\epsilon)=k_t^2\mathbf{g}_t(\mathbf{r},\epsilon) , \tag{31}$$

where

$$k_l^2=\frac{\epsilon^2}{c^2+\epsilon/\rho\{\frac{4}{3}\eta(\epsilon)+\eta^B(\epsilon)\}} \tag{32}$$

and

$$k_t^2=\frac{\epsilon\rho}{\eta(\epsilon)} . \tag{33}$$

The general forms of g_l and $\mathbf{g}_t$ that couple to the particle average velocity $\overline{\mathbf{V}}(t)$ linearly are

$$g_l(\mathbf{r},\epsilon)=h_l(r,\epsilon)\hat{\mathbf{n}}\cdot\overline{\mathbf{V}}(\epsilon) , \tag{34}$$

$$\mathbf{g}_t(\mathbf{r},\epsilon)=h_t(r,\epsilon)\hat{\mathbf{n}}\times\overline{\mathbf{V}}(\epsilon) , \tag{35}$$

where $\hat{\mathbf{n}}$ is the unit vector of position vector $\mathbf{r}$. For these forms of g_l and $\mathbf{g}_t$ to be solutions to the Helmholtz equations [Eqs. (30) and (31)], h_l and h_t should be the modified spherical Bessel functions of the second kind and of the first order [7]. Therefore,

$$g_l(\mathbf{r},\epsilon)=A(\epsilon)\left[\frac{1}{k_l^2r^2}+\frac{1}{k_l r}\right]e^{-k_l r}\hat{\mathbf{n}}\cdot\overline{\mathbf{V}}(\epsilon) \tag{36}$$

and

$$\mathbf{g}_t(\mathbf{r},\epsilon)=B(\epsilon)\left[\frac{1}{k_t^2r^2}+\frac{1}{k_tr}\right]e^{-k_tr}\hat{\mathbf{n}}\times\bar{\mathbf{V}}(\epsilon)\ . \tag{37}$$

In terms of Eqs. (36) and (37), $\mathbf{u}(\mathbf{r},\epsilon)$ is obtained

$$\mathbf{u}(\mathbf{r},\epsilon)=k_l^{-2}\nabla g_l(\mathbf{r},\epsilon)-k_t^{-2}\nabla\times\mathbf{g}_t(\mathbf{r},\epsilon)\ . \tag{38}$$

For complete determination of the flow field $\mathbf{u}(\mathbf{r},t)$, it is necessary to find $A(\epsilon)$ and $B(\epsilon)$ in Eqs. (36) and (37) from the generalized boundary condition Eq. (13), which can be written as coupled linear equations

$$\frac{\alpha K_0}{G}[A(\epsilon)(R+a)(x_l^{-4}+x_l^{-3})e^{-x_l}-B(\epsilon)(R+a)(x_t^{-4}+x_t^{-3}+x_t^{-2})e^{-x_t}-1]$$
$$=-2A(\epsilon)(3x_l^{-4}+3x_l^{-3}+x_l^{-2})e^{-x_l}+B(\epsilon)(6x_t^{-4}+6x_t^{-3}+3x_t^{-2}+x_t^{-1})e^{-x_t}\ , \tag{39}$$

$$\frac{\alpha K_0}{G}[-A(\epsilon)(R+a)(3x_l^{-4}+3x_l^{-3}+x_l^{-2})e^{-x_l}+B(\epsilon)(R+a)(3x_t^{-4}+3x_t^{-3}+x_t^{-2})e^{-x_t}]$$
$$-\frac{\alpha K_1}{G}[A(\epsilon)(R+a)(2x_l^{-4}+2x_l^{-3}+x_l^{-2})e^{-x_l}-B(\epsilon)(R+a)(2x_t^{-4}+2x_t^{-3})e^{-x_t}+1]$$
$$=A(\epsilon)(18x_l^{-4}+18x_l^{-3}+\tfrac{22}{3}x_t^{-2}+\tfrac{4}{3}x_t^{-1})e^{-x_t}-B(\epsilon)(18x_t^{-4}+18x_t^{-3}+7x_t^{-2}+x_t^{-1})e^{-x_t}$$
$$+\frac{c^2\rho/\epsilon+\eta^B(\epsilon)}{\eta(\epsilon)}A(\epsilon)(x_l^{-2}+x_l^{-1})e^{-x_l}\ , \tag{40}$$

where

$$x_l(\epsilon)=k_l(\epsilon)(R+a)$$

and

$$x_t(\epsilon)=k_t(\epsilon)(R+a)\ .$$

IV. VELOCITY AUTOCORRELATION FUNCTION (VAF) OF PARTICLE

Once we determine the velocity field $\mathbf{u}(\mathbf{r},t)$ of background polymers, we can calculate the average force acting on the particle by integrating the stress over the outer boundary surface, which is

$$\mathbf{F}(\epsilon)=-\oint_{S_0}\vec{\sigma}(\mathbf{r},\epsilon)\cdot\hat{\mathbf{n}}\,dS$$
$$=\alpha\psi(\epsilon)\oint_{S_0}\vec{\mathbf{K}}\cdot\{\mathbf{u}(\mathbf{r},\epsilon)-\bar{\mathbf{V}}(\epsilon)\}dS\ . \tag{41}$$

The second equality in the above equation is due to Eq. (13). The result of the calculation is given as

$$\mathbf{F}(\epsilon)=-\zeta(\epsilon)\bar{\mathbf{V}}(\epsilon)\ , \tag{42}$$

with the frequency-dependent friction coefficient

$$\zeta(\epsilon)=\frac{-4\pi\eta(\epsilon)(R+a)^2}{3}\left[2B(\epsilon)(x_t^{-2}+x_t^{-1})e^{-x_t}+A(\epsilon)(x_l^{-2}+x_l^{-1})e^{-x_l}\left\{\frac{4}{3}+\frac{c^2\rho/\epsilon+\eta^B(\epsilon)}{\eta(\epsilon)}\right\}\right]\ , \tag{43}$$

where A and B are determined from the boundary condition, Eqs. (39) and (40).

The equation of motion for the particle can be written as the generalized Langevin equation

$$M\frac{d}{dt}\mathbf{V}(t)=-\int_0^t dt'\zeta(t-t')\mathbf{V}(t')+\mathbf{f}(t)\ . \tag{44}$$

The $\zeta(t)$ is the memory function obtained as the inverse Laplace transform of Eq. (43), $\mathbf{f}(t)$ is the stochastic force [rapidly varying chain segmental force which is not included in the frictional force [Eq. (42)], and M is the particle mass. For the velocity autocorrelation function (VAF) of the particle defined as

$$C(t)=\tfrac{1}{3}\langle\mathbf{V}(t)\cdot\mathbf{V}(0)\rangle\ , \tag{45}$$

where $\langle\ \rangle$ is the average over an equilibrium ensemble. We note $\langle\mathbf{f}(t)\cdot\mathbf{V}(0)\rangle=0$ to obtain

$$M\frac{\partial}{\partial t}C(t)=-\int_0^t dt'\zeta(t-t')C(t')\ . \tag{46}$$

Then one obtains the Laplace transform of the VAF

$$C(\epsilon)=\frac{\frac{1}{3}\langle V^2\rangle}{\epsilon+\zeta(\epsilon)/M}=\frac{k_BT/M}{\epsilon+\zeta(\epsilon)/M} \tag{47}$$

and the associated Fourier transform, called the power spectrum,

$$C(\omega)=2\,\mathrm{Re}\frac{k_BT/M}{-i\omega+\zeta(\epsilon=-i\omega)/M}\ . \tag{48}$$

Inserting Eq. (43) into Eq. (48) and inverse-Fourier transforming the latter, we finally obtain VAF $C(t)$.

The long-time behavior of VAF

The explicit analytic expression for $C(\omega)$ for arbitrary frequencies is too complicated to be presented, but will be given only for the limiting cases of low frequencies and high frequencies. At low frequencies, the dominant contribution to $\zeta(\epsilon)$ is expanded in powers of $\epsilon^{1/2}$

$$\zeta(\epsilon)=\zeta_0(1+g_{1/2}\epsilon^{1/2}+g_1\epsilon+g_{3/2}\epsilon^{3/2}+\cdots) . \quad (49)$$

The first term is the zero-frequency friction coefficient corresponding to the steady-state friction coefficient obtained earlier by us [5]

$$\zeta_0=\frac{\zeta_h\zeta_e}{\zeta_h+\zeta_e} , \quad (50)$$

where

$$\zeta_h=6\pi\eta_0(R+a)\left[1-\frac{K_1}{K_0(6+\gamma)+K_1(3+\gamma)}\right] , \quad (51)$$

$$\zeta_e=4\pi(R+a)^2\alpha\tau_D\left[K_0+\frac{2+\gamma}{6+\gamma}K_1\right] . \quad (52)$$

In the above, $\gamma=K_0\alpha\tau_D(R+a)/\eta_0=R/R_c$, $R_c\equiv G/\alpha K$, $\eta_0=G\tau_D$ is the zero-frequency shear viscosity and all the other parameters are already introduced in Sec. II. As discussed earlier, the friction coefficient recovers, in the large-particle limit $\gamma\to\infty$ the Stokes friction

$$\zeta_0\to\zeta_h\to 6\pi\eta_0 R \quad (53)$$

of the usual hydrodynamics using no-slip boundary condition (BC). On the other hand for small-particle limit $\gamma\to 0$ it approaches to a reasonable expression

$$\zeta_0\to\zeta_e\to 4\pi(R+a)^2\alpha\tau_D(K_0+\tfrac{1}{3}K_1)\equiv K_s\tau_D , \quad (54)$$

which is just the friction due to the elastically effective surface chains attached to the particle. Equation (54) defines the overall spring constant K_s of the elastic force on the particle by ESCs.

The next higher order term

$$g_{1/2}=\frac{1}{6\pi}\zeta_0\rho^{1/2}\eta_0^{-3/2} \quad (55)$$

in $\zeta(\epsilon)$ [Eq. (49)] contributes to the $C(\omega)$ [Eq. (48)] for low frequencies

$$C(\omega)\simeq\frac{2k_BT}{\zeta_0}(1-\sqrt{2}g_{1/2}\omega^{1/2}) \quad (56)$$

yielding, upon inverse-Fourier transformation, the long-time analytic behavior,

$$C(t)\simeq\frac{k_BT}{\rho}(\nu t)^{-3/2} \quad \text{as } t\to\infty , \quad (57)$$

where $\nu=\eta_0/\rho$ is kinematic viscosity. The above long-time tail is a universal feature arising from the viscous hydrodynamic backflow in the form of vortex [8] but it is remarkable that, because of the very high viscosity $\eta_0\sim N^\delta$, the tail is much weaker compared with that of a particle in a small-molecule fluid. This feature is contrary to the expectation one might (falsely) have that the disengagement via reptation gives rise to a sustained long-time tail, in a liquid of entangled polymers. What happens, in fact, is that the highly viscous background damps the propagation of large-scale hydrodynamic feedback to a very feeble level. This feature of entanglement constraint effect regardless of particle size and mass becomes more obvious when the higher terms $g_1, g_{3/2}, \ldots$ in $\zeta(\epsilon)$ [Eq. (49)] are considered as below.

It suffices to discuss the cases $R\gg a$ where g_1 and $g_{3/2}$ can be reduced to relatively simple forms

$$g_1=-\tau_D-\frac{\zeta_0}{12\pi R\rho c^2}+\frac{2\pi\rho R^3}{3\zeta_0} \quad (58)$$

$$g_{3/2}=-\frac{\pi}{12}\rho^{1/2}\eta^{-3/2}\tau_D\zeta_0\left[1+2\frac{c_t^2}{c^2}\right] . \quad (59)$$

Here $c_t=(G/\rho)^{1/2}$. The last term of Eq. (58) represents the effect of buoyance (or virtual mass) noted by Boussinesq in 1903 [9] in an incompressible Newtonian fluid. While this term tends to reduce M by half the mass of liquid displaced by the particle and thus enhance particle mobility, the other two (negative) terms characteristic of compressible polymer liquids retard it. The latter, which is proportional to viscosity, predominates for most of the cases where the particle is not extraordinarily large. The term $g_{3/2}$ gives rise to a long-time tail of $t^{-5/2}$

$$C(t)'\sim\frac{k_BT}{\rho}\left[\frac{t}{\tau_D}\right]^{-1}(\nu t)^{-3/2} . \quad (60)$$

Again, as discussed before, this tail is also suppressed because of its dependence on viscosity. All in all, the long-time behaviors we found here imply that the polymer entanglements retard the particle motion enormously even after the reptation time.

The short-time approximation and comparison with the numerical results

The strong decay of VAF at long times as revealed in our results suggests that the relaxation dynamics of the particle is governed predominantly by its short-time behavior. This is indeed supported by Figs. 2 and 3 (full curves) which represent the numerical results of our model theory for large particle $R=10^4R_s$ and small particle $R=10R_s$, respectively.

We took the numerical values from the experimental data for polystyrene melt at 200 °C which is well above its glass transition temperature: the mean number of monomers between the entanglement $N_e=174$, the primitive chain length $R_e=92$ Å, Kuhn step length $b\simeq 7$ Å, Rouse friction coefficient $\zeta_1\simeq 1.12\times10^{-7}$ dyn sec/cm, plateau modulus $G\simeq 2.67\times10^6$ dyn/cm^2, reptation time $\tau_D\simeq 4\times10^{-12}N^3$ sec, the steady-state viscosity $\eta=1.08\times10^{-5}N^3$ dyn sec/cm^2. To see the trends, we tentatively considered $N=10^4$ and put the particle mass density ρ_p

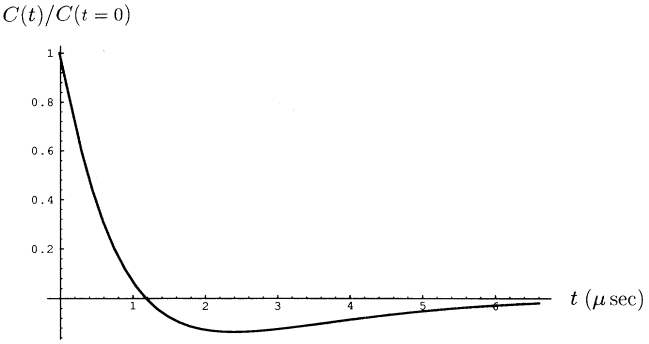

FIG. 2. The VAF $C(t)$ of a large particle ($R=10^4R_s$ or $\gamma\simeq 100$). See the text for the other parameters involved.

to be same as the polymer liquid density in the bulk which we put as $\rho=1$ g/cm^3 and, for the boundary layer parameters $R_s=R_e$ and $\alpha\simeq(1/7.76)R_e^{-2}$.

With variables chosen this way, Fig. 2 pertains to the case of the large particle with $\gamma\simeq 100$, where the Stokes friction [Eq. (53)] applies. In this case the VAF shows a decay to the negativity leading to a caging effect at short times (much shorter than τ_D). This is not much different except for the time scale from the hydrodynamic result of Zwanzig and Bixon [6] for an atom in simple fluid. The behaviors of VAF as shown in Fig. 2 appear to be typical of the particle of all but small sizes. Figure 3 (solid curve) is the case of the small particle with $\gamma=0.1$. Since $\rho=\rho_p$, this case pertains to the very light particle. Unlike in Fig. 2, the VAF is characterized by the rapid oscillations which is underdamped at times much shorter than τ_D.

As an attempt to understand the physics behind the short-time behaviors of VAF analytically, we determine the high frequency dynamic friction coefficient by expanding the bracket in Eq. (43) to the order linear in ϵ^{-1} assuming $\epsilon\tau_s\gg 1$

$$\zeta(\epsilon)\simeq\frac{\eta(\epsilon)}{G}K_s[1-(\epsilon\tau_s)^{-1}]$$
$$\simeq\frac{\eta(\epsilon)}{G}K_s\frac{1}{1+(\epsilon\tau_s)^{-1}}\ . \tag{61}$$

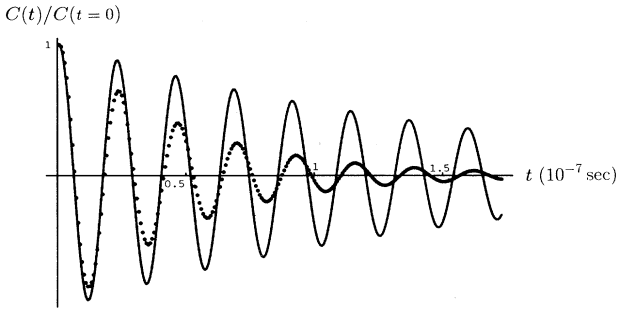

FIG. 3. The VAF $C(t)$ of a small particle ($R=10R_s$ or $\gamma\simeq 0.1$). See the text for the other parameters involved. [Dotted curve is the short-time approximation, Eq. (66).]

Here K_s is the overall spring constant defined by Eq. (54). The τ_s is given by

$$\tau_s^{-1}=\frac{\alpha K}{G}\left[\frac{G}{\rho}\right]^{1/2}\left[\tfrac{1}{2}+\left[\tfrac{4}{3}+\frac{c^2\rho+G^B}{G}\right]^{-1/2}\right]$$
$$=\frac{1}{R_c}c_t[\tfrac{1}{2}+c_tc_l^{-1}]\ , \tag{62}$$

where

$$c_l=\left[c^2+\frac{\frac{4}{3}G+G^B}{\rho}\right]^{1/2}\ , \tag{63a}$$

$$c_t=\left[\frac{G}{\rho}\right]^{1/2} \tag{63b}$$

are the longitudinal and transverse sound velocities and

$$R_c\equiv\frac{G}{\alpha K}=\gamma^{-1}R$$

is a crossover distance introduced earlier.

In getting these expressions, we assumed that, as in the cases with Figs. 2 and 3, the size of the particle is much larger than the boundary layer ($R\gg a$) so that we have $K_0\simeq K_1=K$ [Eq. (5)]. The many usual situations of the colloidal particles with $R>0.1$ μ and $a\lesssim 100$ Å satisfy this condition. For the short-time regime we consider here, the polymer chains remain entangled and thus act collectively as an elastic solid. The relaxation modulus $\eta(t)=G\psi(t)$ is nearly flat for $t>\tau_e$ with the time of the plateau region in the order of $\tau_D\sim N^{\delta}$, so we may replace, without appreciable errors, $\eta(\epsilon)$ by

$$\eta(\epsilon)=\frac{G}{\epsilon+\tau_D^{-1}}\ . \tag{64}$$

Inserting Eq. (61) with Eq. (64) to Eq. (47), we obtain, for $(\epsilon\tau_s)^{-1}\ll 1$, the Laplace transform

$$C(\epsilon)=k_BT/\frac{M}{\epsilon+\frac{K_s/M}{\epsilon+\tau^{-1}}}\ . \tag{65}$$

Here, $\tau^{-1}=\tau_s^{-1}+\tau_D^{-1}$, which can be replaced by τ_s^{-1} since $\tau_D\gg\tau_s$. Equation (65) is in the form of a continued fraction representation truncated at the second order. As well known in the theories of simple systems [10], this representation is a choice method for describing the short-time dynamics. Equation (65) is identical in form to the model of Berne, Boon, and Rice for an atom in dense simple liquids where the elastic constant K_s is given in terms of the interatomic potential [11].

Upon an inverse Laplace transform of Eq. (65) the VAF is obtained as

$$C(t)=\frac{k_BT}{M}[\cos\Omega t+\tfrac{1}{2}(\Omega\tau_s)^{-1}\sin\Omega t]e^{-t/2\tau_s}\ , \tag{66}$$

where

$$\Omega=(\omega_0^2-\tfrac{1}{4}\tau_s^{-2})^{1/2} \tag{67}$$

involving the natural frequency of oscillation

$$\omega_0=\left[\frac{K_s}{M}\right]^{1/2} .$$

In order to appreciate the underdamped oscillation of $C(t)$, let us consider the limit $\epsilon\rightarrow\infty$, in which

$$\zeta(\epsilon)=\frac{K_s}{\epsilon}$$

and the force [Eq. (42)] becomes an elastic one induced by a displacement $\delta\mathbf{X}$ of the particle,

$$\mathbf{F}(t)=-K_s\delta\mathbf{X}(t) . \tag{68}$$

Then the VAF is given as

$$C(\epsilon)=\frac{k_BT/M}{\epsilon+\dfrac{K_s/M}{\epsilon}} , \tag{69}$$

whose inverse transformation yields undamped oscillator behavior for $C(t)$ with the frequency ω_0. This means that the instantaneous response of the background polymers to the particle set into motion at $t=0$ is the elastic force with the spring constant K_s [Eq. (54)] provided by its immediate neighbors, namely, ESCs.

In a short-time interval, $0<t\lesssim\tau_s$, the response from the more distant chains, which are still elastic since they remain entangled, comes into play to affect particle motion. A close examination of Eq. (62) reveal that τ_s is about the time during which the transverse sound passes the crossover distance $R_c=G/\alpha K$. During this short traversal time, the local disturbance (sound wave) such as compression at the front and expansion at the rear of particle are incurred over the distance $\sim R_c$. The short-time solution of $\mathbf{u}(\mathbf{r},t)$ obtained from Eq. (38) is

$$\mathbf{u}(\mathbf{r},t)=\gamma\left[\frac{c_t}{r}\{\overleftrightarrow{1}-\mathbf{nn}\}\cdot\delta\mathbf{X}\left[t-\frac{r-R}{c_t}\right]+\frac{2c_l}{r}\mathbf{nn}\cdot\delta\mathbf{X}\left[t-\frac{r-R}{c_t}\right]\right] . \tag{70}$$

Thus the disturbance at $\mathbf{r}$ is delayed by the time which the sound takes to traverse from the particle to point $\mathbf{r}$. This delayed response yields a memory effect on the part of the particle, a damping on its motion. The correlation function is obtained by inserting Eq. (61) to Eq. (47)

$$\frac{\partial C(t)}{\partial t}=-\omega_0^2\int_0^t dt'\exp\left[-\frac{(t-t')}{\tau_s}\right]C(t') . \tag{71}$$

The damping couples with the oscillation of natural frequency ω_0, leading to the underdamped oscillation behavior for $C(t)$, as observed in Eq. (66).

Shown in Figs. 4 and 5 are the power spectra $C(\omega)$ of the two cases considered in Figs. 2 (large particle) and 3 (small particle), respectively. The dotted curves are the first order high frequency approximation [Eq. (66)]. For frequencies higher than the peak frequency $\omega\sim10^8$ sec^{-1}, the approximation appears to be valid for the small particle (Fig. 5). This is reflected in Fig. 3 where the approximation (dotted curve) for $t\lesssim10^{-8}$ sec is shown to be in a close agreement and for other time regimes a reasonable agreement with the full theory. On the other hand for the large particle (Fig. 4), the agreement is reached for high frequencies $\omega\gtrsim10^8$ sec^{-1}. For $C(t)$ (Fig. 2), the approximation is only valid for $t\lesssim10^{-8}$ sec which is too short a time region to be seen here in $C(t)$.

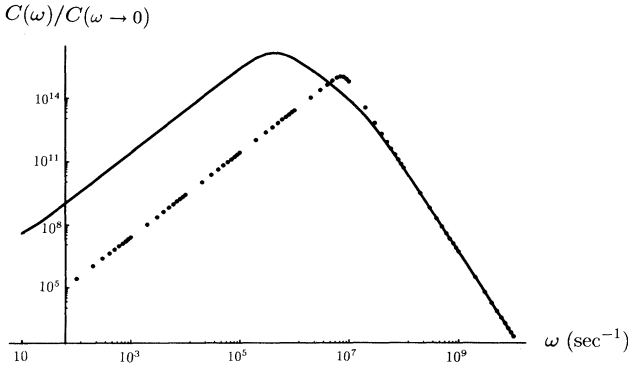

FIG. 4. The power spectrum of the VAF (large particle) given in Fig. 2. [Dotted curve is from the short-time approximation, Eq. (65).]

Why does the approximation Eq. (66) yield a reasonable result for the small particle while it does not for the large particle except for a very short time? Recall that the approximation is valid for $\omega\tau_s\gg1$. For a small particle it is easy to understand the short-time response of the chains in its vicinity plays the dominant role in affecting its dynamics, i.e., underdamped harmonic motion. But for the larger particle, the response from the background is more long ranged involving more distant chains for longer time. Furthermore, the large particle in our case means heavy particle, for which it is shown that the oscillation frequency Ω [Eq. (67)] tends to be suppressed.

With more terms in $(\epsilon\tau_s)^{-1}$ expansion we can expect to achieve the better convergence, because VAF is governed essentially by short-time dynamics with $t\ll\tau_D$.

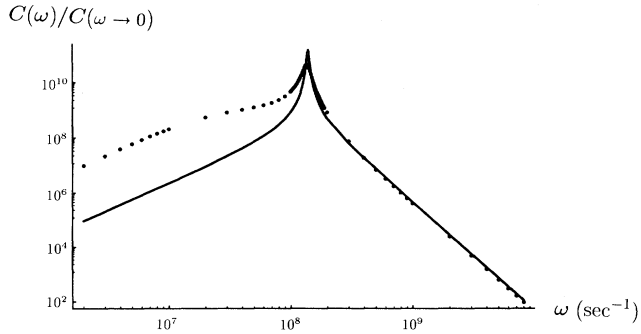

FIG. 5. The power spectrum of the VAF (small particle) given in Fig. 3. [Dotted curve is from the short-time approximation, Eq. (65).]

Therefore it seems reasonable to say that the caging of a particle, regardless of its size, is enhanced by the sound wave of the surrounding elastic media on various scales.

Diffusion constant: interplay of short-time and long-time dynamics

The diffusion constant D of the particle is given by $C(\epsilon \to 0)$ [Eq. (47)]

$$D = \frac{k_B T}{\zeta_0} \quad \text{(Einstein relation)}$$
$$= \int_0^\infty dt C(t) \ . \tag{72}$$

From the ζ_0 [Eq. (50)], we find

$$D = D_h + D_e \ , \tag{73}$$

where

$$D_h = \frac{k_B T}{\zeta_h}, \quad D_e = \frac{k_B T}{\zeta_e} \ .$$

This additivity, as well as the limiting behaviors of the diffusion constant, was discussed in our earlier work [3]. Now with the VAF at hand, these features can be better appreciated.

For a particle very small $\gamma \ll 1$ the diffusion constant has the limiting behavior

$$D \to D_e = \frac{k_B T}{\zeta_e}$$
$$\to \frac{k_B T}{K_s \tau_D} \ , \tag{74}$$

in accordance with Eq. (54). This is entirely from the elastically effective surface chains, the immediate neighbors to the particle, which are disengaged during the time τ_D. The VAF satisfies the equation

$$\frac{\partial C(t)}{\partial t'} = -\omega_0^2 \int_0^t dt' \psi(t-t') C(t') \tag{75}$$

and, since $\omega_0 \equiv \sqrt{K_s/M} \gg \tau_D^{-1}$, has the oscillatory behavior with slow damping: using an approximation $\psi(t) = e^{-t/\tau_D}$ consistent with Eq. (64),

$$C(t) \simeq \frac{k_B T}{M} \cos(\omega_0 t) e^{-t/2\tau_D} \ . \tag{76}$$

In this case of $\gamma \ll 1$, the disturbance from the more distant chains in the background is vanishingly small as implied in its short-time behavior [Eq. (70)]. For the large particles, however, the response from the more distant chains becomes important. In the case of a very large particle, $\gamma \gg 1 (R \gg R_c = G/\alpha K)$, we obtain the Stokes-Einstein diffusion

$$D \to D_h = \frac{k_B T}{6\pi\eta R} \ .$$

In this case, the diffusivity is entirely irrelevant to the details of particle-polymer interface, but is determined by the hydrodynamics using a no-slip BC. (It should be noted that this case precludes the large particle with a very small α in which γ is not very large. What happens in the latter case is the slippage of flow of entangled polymers on particle surface [12–14].) As discussed before, the change of VAF is largely governed by short-time dynamics but, interesting enough, the time integral which determines diffusivity is mostly from long-time domain. This is due to the fact that, at long times, despite its very small magnitude, $C(t)$ is characterized by the enormously slow decay.

For the intermediate particle sizes, the diffusion constant appears as the sum of two contributions D_e and D_h [Eq. (73)]. What underlies in this remarkable additivity is that the two modes of dynamical processes mentioned above for the two limiting cases are operative on distinct time scales. Thus one can decompose $\mathbf{V}(t)$

$$\mathbf{V}(t) \simeq \mathbf{V}_e(t) + \mathbf{V}_h(t) \tag{77}$$

into two contributions from short-time ESC effect, $\mathbf{V}_e(t)$ and long-time hydrodynamic effect, $\mathbf{V}_h(t)$. Since $\mathbf{V}_h(t)$ varies slowly compared and does not correlate with $\mathbf{V}_e(t)$, the VAF is approximately given as

$$C(t) \simeq C_e(t) + C_h(t) \ , \tag{78}$$

where

$$C_e(t) = \tfrac{1}{3} \langle \mathbf{V}_e(t) \cdot \mathbf{V}_e(0) \rangle \ , \tag{79}$$

$$C_h(t) = \tfrac{1}{3} \langle \mathbf{V}_h(t) \cdot \mathbf{V}_h(0) \rangle \ . \tag{80}$$

The time integration of Eq. (78) yields indeed the diffusivity in additive form [Eq. (73)].

V. SUMMARY AND CONCLUSION

In investigating the dynamics of the particle in melt of entangled polymers, we employed the microscopic boundary model, which, briefly recapitulated in Sec. II, enables us to calculate the dynamic response of the background polymers to the particle motion. According to the model, the short-range response is described by statistical dynamics of the elastically effective surface chains attached on the particle and engaged to the entanglements, which are coupled to the long-range dynamic response of the more distinct chain described as a viscoelastic continuum. Using this generalized hydrodynamic scheme, we obtained the velocity autocorrelation function (VAF), which has been analyzed in depth for long-time and short-time regimes. In the long times, the VAF has the long tail $t^{-3/2}$ and $t^{-5/2}$ with positive amplitudes which are significantly suppressed by entanglement constraints. In the short time, the polymers respond to an elastic solid due to the constraints, and the theory shows delayed distortion of the elastic media near the particle tends to enhance caging. The dominant variation in VAF occurs only at short times $t \lesssim \tau_D$, whether it is underdamped oscillation as found for the small particle (Fig. 3) or it is like Fig. 2 as found for the large particle.

For the time integral of VAF, which is a diffusion constant, however, the long-time effect is found to be significant; for a particle much larger than the crossover

length R_c, the diffusivity is the Stokes-Einstein hydrodynamic result of the usual no-slip B.C., which is entirely insensitive to microscopic details of interface and short-time dynamics and thus affected largely by long-time behavior. For a small particle, the diffusion constant is largely given by the effect (disengagement) of interface chains. For an intermediate particle, the interplay of short-time and long-time dynamics is found to yield the diffusivity as the sum of each contribution. The generalized hydrodynamic scheme developed here can also be extended to the more complex situations involving chain segmental fluctuations and solvent dynamics. The general ideas derived in this work, namely, the long-time hydrodynamic feedback yielding long-time tails as well as short-time surface chains and sound wave effects leading to enhanced caging will retain their validity.

In conclusion, the microscopic boundary layer model provides a tractable and powerful analytical method for studying the dynamics of particles coupled to the entangled polymers on various time scales. The model shows that the short-time dynamical effects of the chains adsorbed on the particle became more important as the particle gets smaller. The particle can be a sensitive probe to the dynamics of the polymers, which shows an unusual interplay of elastic response at short times and viscous relaxation via reptation of the polymer chains at long times.

ACKNOWLEDGMENTS

This work was supported in part by RIST, as well as BRSC and CAMP of POSTECH, each funded by Ministry of Education of Korea and KOSEF. Stimulating discussions with Y. H. Jeong are gratefully acknowledged.

[1] P. G. de Gennes, J. Chem. Phys. **55**, 572 (1971).
[2] M. Doi and S. F. Edwards, *The Theory of Polymer Dynamics* (Oxford University Press, Oxford, 1986).
[3] W. Sung, in *Physics of Complex Fluids and Biological Systems,* edited by W. Sung *et al.* (Min Eum Sa Co, Seoul, 1993).
[4] H. A. Bethe, Proc. Roy. Soc. (London) A **150**, 552 (1935).
[5] W. Sung and Min Gyu Lee (unpublished).
[6] R. Zwanzig and M. Bixon, Phys. Rev. A **2**, 2005 (1970).
[7] P. M. Morse and H. Feshbach, *Methods of Theoretical Physics* (McGraw-Hill, New York, 1963).
[8] B. J. Alder and T. E. Waingwright, Phys. Rev. Lett. **18**, 988 (1967); M. H. Ernst, E. H. Hauge, and J. M. J. Van Leeuven, Phys. Rev. A **4**, 2005 (1971).
[9] L. D. Landau and E. M. Lifshitz, *Fluid Dynamics* (Addison-Wesley, Reading, MA, 1959).
[10] J. P. Boon and S. Yip, *Molecular Hydrodynamics* (McGraw-Hill, New York, 1980).
[11] B. J. Berne, J. P. Boon, and S. A. Rice, J. Chem. Phys. **45**, 1086 (1966).
[12] W. Sung (unpublished).
[13] P. G. de Gennes, C. R. Acad. Sci. (Paris) B **288**, 219 (1979).
[14] A. Ajdari, F. Brochard, P. G. de Gennes, L. Leibler, J-L. Viory, and M. Lubinstein, Physica A **204**, 17 (1994).